

Effect of carbonaceous nanoadditions on strain sensing and heating functions in cement pastes

B. del Moral¹ , C. Farcas¹ , O. Galao¹ , F. J. Baeza¹ , E. Zornoza¹ , P. Garcés^{1*} 

*Contact author: pedro.garces@ua.es

DOI: <https://doi.org/10.21041/ra.v14i1.713>

Received: 04/11/2023 | Received in revised form: 12/12/2023 | Accepted: 19/12/2023 | Published: 01/01/2024

ABSTRACT

In this research, the use of conductive nanoadditions, such as carbon nanotubes (CNT) and graphite products (GP), in cement specimens has been studied to develop strain sensing and heating functions. For this purpose, cement paste specimens with addition of 1% CNT and 5% GP have been fabricated and heating tests have been performed in direct current (DC) and alternating current (AC) at 20 V and 40 V. In addition, the influence of temperature on the strain sensing tests in the range from 0 °C to 60 °C has been studied, obtaining good results in both techniques. Therefore, these materials offer a very interesting alternative in structural monitoring and may have applications in the heating of infrastructures such as bridges and airports, avoiding the use of corrosive substances.

Keywords: nanoadditions; strain sensing; cement pastes; heating; resistivity.

Cite as: del Moral, B., Farcas, C., Galao, O., Baeza, F. J., Zornoza, E., Garcés, P. (2024), “*Effect of carbonaceous nanoadditions on strain sensing and heating functions in cement pastes*”, Revista ALCONPAT, 14 (1), pp. 13 – 24, DOI: <https://doi.org/10.21041/ra.v14i1.713>

¹Departamento de Ingeniería Civil, Escuela Politécnica Superior, Universidad de Alicante, España.

Contribution of each author

In this work Beatriz del Moral Delgado contributed to the activity of the development of the experimental program (35%) and data processing (20%). Catalina Farcas contributed to the activity of the development of the experimental program (35%) and data processing (20%). Oscar Galao Malo contributed to the experimental program planning (25%), experimental program development activity (10%) and data processing (15%). Francisco Javier Baeza de los Santos contributed to the planning of the experimental program (25%), contributed to the development activity of the experimental program (10%) and data processing (15%). Emilio Zornoza contributed to the planning of the experimental program (25%), contributed to the activity of the development of the experimental program (5%) and data processing (15%). Pedro Garcés contributed to the planning of the experimental program (25%), contributed to the development activity of the experimental program (5%) and data processing (15%).

Creative Commons License

Copyright 2022 by the authors. This work is an Open-Access article published under the terms and conditions of an International Creative Commons Attribution 4.0 International License ([CC BY 4.0](https://creativecommons.org/licenses/by/4.0/)).

Discussions and subsequent corrections to the publication

Any dispute, including the replies of the authors, will be published in the third issue of 2024 provided that the information is received before the closing of the second issue of 2024.

Efecto de las nanoadiciones carbonosas en las funciones de percepción de la deformación y calefacción en pastas cementicias

RESUMEN

En esta investigación se ha estudiado el uso de nanoadiciones conductoras, como los nanotubos de carbono (NTC) y productos de grafito (PG), en probetas de cemento para desarrollar las funciones de percepción de la deformación y calefacción. Para ello, se han fabricado probetas de pasta de cemento con adición de 1% NTC y 5% PG y se han realizado ensayos de calefacción en corriente continua (DC) y alterna (AC) a 20 V y 40 V. Además, se ha estudiado la influencia de la temperatura en los ensayos de percepción de la deformación en rangos comprendidos entre 0 °C y 60 °C, obteniéndose buenos resultados en ambas técnicas. Por tanto, estos materiales ofrecen una alternativa muy interesante en la monitorización estructural y pueden tener aplicaciones en la calefacción de infraestructuras como puentes y aeropuertos, evitando el uso de sustancias corrosivas.

Palabras clave: nanoadiciones; percepción; pastas de cemento; calefacción; resistividad.

Efeito de nano adições de base carbono nas funções de deformação e percepção de aquecimento em pastas cimentícias

RESUMO

Nesta pesquisa, foi estudado o uso de nano adições condutoras, como nanotubos de carbono (CNT) e produtos de grafite (PG), em corpos de prova de cimento para desenvolver as funções de detecção de deformação e aquecimento. Para tanto, foram fabricados corpos de prova de pasta de cimento com adição de 1% de CNT e 5% de PG e realizados ensaios de aquecimento em corrente contínua (CC) e corrente alternada (CA) em 20 V e 40 V. Além disso, foi estudado a influência da temperatura em testes de percepção de deformação em faixas entre 0 °C e 60 °C, obtendo bons resultados em ambas as técnicas. Portanto, estes materiais oferecem uma alternativa muito interessante na monitorização estrutural e podem ter aplicações em infraestruturas de aquecimento como pontes e aeroportos, evitando a utilização de substâncias corrosivas.

Palavras-chave: nano adições; percepção; pastas de cimento; aquecimento; resistividade.

Legal Information

Revista ALCONPAT is a quarterly publication by the Asociación Latinoamericana de Control de Calidad, Patología y Recuperación de la Construcción, Internacional, A.C., Km. 6 antigua carretera a Progreso, Mérida, Yucatán, 97310, Tel.5219997385893, alconpat.int@gmail.com, Website: www.alconpat.org

Reservation of rights for exclusive use No.04-2013-011717330300-203, and ISSN 2007-6835, both granted by the Instituto Nacional de Derecho de Autor. Responsible editor: Pedro Castro Borges, Ph.D. Responsible for the last update of this issue, ALCONPAT Informatics Unit, Elizabeth Sabido Maldonado.

The views of the authors do not necessarily reflect the position of the editor.

The total or partial reproduction of the contents and images of the publication is carried out in accordance with the COPE code and the CC BY 4.0 license of the Revista ALCONPAT.

1. INTRODUCTION

Structural monitoring systems have been developed to oversee the performance of structures, aiming to ensure their safety and appropriate lifespan, as well as to optimize rehabilitation interventions (Baeza et al., 2018). Despite the varied typologies of strain sensors (piezoelectric ceramic sensors, fiber optic sensors, or strain gauges), their durability remains limited (Li et al., 2004; Song et al., 2006). However, conductive cement sensors have emerged as a promising alternative and can be easily obtained by incorporating a conductive additive, such as carbon fibers (CF), nanofibers (CNF), or nanotubes (CNT), into the cementitious matrix (Camacho-Ballesta et al., 2016; Han et al., 2015). The integration of these conductive additions enhances the electrical conductivity of cement, enabling it to function as a strain sensor. By measuring changes in electrical resistance, the sensor can detect stress and deformation within the structure. The ability to correlate material resistivity changes with deformation makes them undoubtedly interesting for structural monitoring purposes. This property, commonly known as strain sensing, has been extensively explored in recent years (Baeza et al., 2013a, 2013b; Chung, 1998; Galao et al., 2014; Ubertini et al., 2014, 2016).

The inclusion of a conductive material enhances the electrical conductivity of the composite, transforming it into a multifunctional material applicable to various concrete functions, such as de-icing or serving as an anode in electrochemical techniques (Carmona et al., 2015; del Moral et al., 2013). One of the most powerful and current functions that a conductive cementitious material can perform is heating. The increase in material temperature is based on the Joule effect when an electric current is applied, where heat is generated by current flowing through a conductor (Ding et al., 2013; Liu et al., 2010). The heat-generating capacity of electrically conductive cementitious materials is associated with their resistance, as expressed by Joule's first law (Wang et al., 2004). By controlling the supplied electrical power, the temperature of the compound can be adjusted. When this concept is applied to structural materials, it becomes possible to use the structural material itself to induce ice melting on its surface (or to prevent its formation). Traditional building heating systems include underground pipes, infrared heat lamps, heated fluids, and solar energy. However, these systems are complex to construct, costly, and lack integration with the original structure, limiting their application (Zhang et al., 2011). Yehia et al. (Yehia et al., 2000) and Chung (Chung, 2004) were pioneers in developing this function using conductive cementitious materials. Multifunctional cement-based compounds maintain high structural integrity with original structures. That is, the damage induced by thermal expansion during heating is insignificant, as their thermal expansion coefficient is similar to that of original cementitious structures (Chung, 2004). The use of these materials in transport infrastructure such as bridges or airports could avoid the use of corrosive salts that may damage steel reinforcements, the concrete itself, and the ecosystem. Therefore, these materials could be viable for increasing the ambient temperature of rooms or for preventing ice formation, or inducing de-icing, in civil engineering infrastructures, among others.

In this research, strain sensing and heating functions have been implemented in cement specimens with conductive nano-additions such as NTC and graphite products.

2. EXPERIMENTAL PROGRAMME

2.1 Fabrication of Conductive Cement Paste Specimens

The materials used in this research were as follows:

- Distilled water.
- CEM I 52.5 R Portland Cement UNE-EN 197-1, supplied by Cemex-Spain S.A. (Alicante).
- Graphite products: Expanded graphite (ABG1010), supplied by Superior Graphite.
- CNT Graphistrength C100 provided by Arkema.
- Superplasticizer Sika Viscocrete 20-HE, supplied by Sika-Spain.

The dispersion process of the nano-additions is essential for the optimal utilization of their properties when integrated into the cement matrix. This process started with the weighing of the CNT under a fume hood. The concentration used during this treatment consisted of 18 grams of CNT per 450 ml of water. Then, the CNT dispersions were prepared using a Robot Coupé blade robot for 10 minutes. The resulting suspension is homogenized, adopting a less liquid consistency similar to a paste. The paste formed by the robot was poured back into the container, collecting all the paste from the robot's walls using a silicone spatula, and the superplasticizer Sika Viscocrete 20-HE was added in a Plastifier/CNT ratio of 0.4. Then, an ultrasonic treatment was applied to the dispersion for 10 minutes using a Hielschier UP400St ultrasonic tip with a 65% amplitude, using an ice bath to avoid excessive increase in the mixture's temperature.

The mixing of the pastes was carried out with a mortar mixer. The prepared dispersions were fully poured into the mixer's container and cement was added in three parts, approximately 600 g each time. Each part was mixed for 2 minutes at low speed. Finally, after all the cement parts were added, the paste was mixed for one more minute at high speed. The water/cement ratio for these pastes formed with a 1% CNT and 5% ABG1010 mix was 0.4.

Next, the cement pastes were poured into standardized molds and compacted using a vibrating table. From each mold, 3 specimens of $4 \times 4 \times 16 \text{ cm}^3$ were produced. Once the fresh paste was levelled in the molds, they were introduced into a humid chamber until the next day (24 hours), when they were extracted for demolding and proper labelling. Subsequently, the specimens continued curing in a humid chamber (100% RH) at 20 °C for 28 days, according to UNE-EN 196-1:2018. After 28 days of curing, mechanical characterization tests were performed on 3 specimens, 6 specimens were instrumented for conductivity and piezoresistivity tests, and 6 specimens were preserved for heating tests.

2.2 Description of strain sensing test in climatic chamber.

Prior to the strain sensing tests, the specimens were instrumented to enable the recording of measurements, using the four-point method. This instrumentation consists of painting four peripheral bands with silver paint (Conductive Silver RS 186-3600 from RS components), on four copper wires, previously wound peripherally according to the scheme in Figure 1.

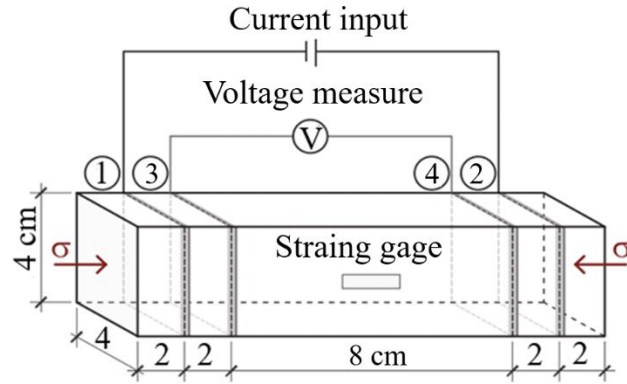


Figure 1. Schematic of the instrumentation of specimens for resistivity tests

The electrodes thus fixed constitute the electrical connections for the application of a predefined electric current between the outer points ① and ② while recording the potential difference measured between the inner points ③ and ④. The electric current was applied using a Keithley 6220 digital source from National Instruments Inc. The potential difference was measured with a Keithley 2002 digital multimeter from National Instruments Inc. The 10 mm strain gauges (model 10/120 CLY41-4L-3M, supplied by HBM) were used to record the deformations caused by both the stress and the temperature increase during the test.

The tests were performed in a mechanical press controlling the load and the speed of its application with a climatic chamber model MUF 401, supplied by Servosis. The air temperature inside this chamber can be controlled within a temperature range of $-10\text{ }^{\circ}\text{C}$ to $150\text{ }^{\circ}\text{C}$. The measurement configuration is represented in the scheme of Figure 2.

In addition to deformations related to the applied stress, the samples underwent additional thermal deformations due to temperature changes. To control this effect, a second control specimen was placed in the climatic chamber. No load was applied to this specimen, but its strain gauge recorded the thermal deformations, which were later subtracted from the measurement of the loaded specimen.

Ambient temperature and the surface temperature of both specimens were measured with Pt-100 type temperature sensors. Additionally, a small borehole was made in the control specimen to install a thermocouple at its center to monitor possible thermal gradients. To limit the effect of water loss related to the heating of the specimen, temperatures were set between $0\text{ }^{\circ}\text{C}$ and $60\text{ }^{\circ}\text{C}$ (with $20\text{ }^{\circ}\text{C}$ increments).

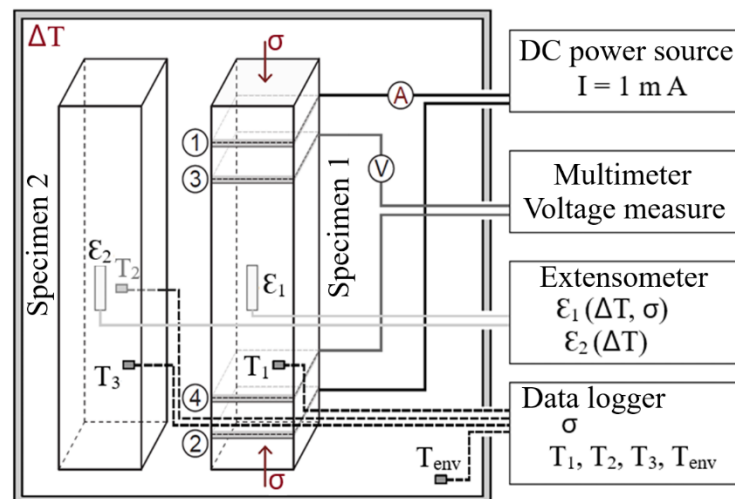


Figure 2. Schematic of the test inside the climatic chamber. (Retrieved from del Moral, B.,2021).

2.3 Description of heating test.

Heating tests were conducted under laboratory conditions, after the curing period. The tests consisted of applying different voltages in alternating and direct current between the two ends of the conductive specimens ($4 \times 4 \text{ cm}^2$). A layer of conductive silver paint was previously applied to improve the electrical contact between the primary electrodes (0.5 mm thick copper plate and 2 mm thick carbon felt) and the cementitious material. The setup can be observed in Figure 3.

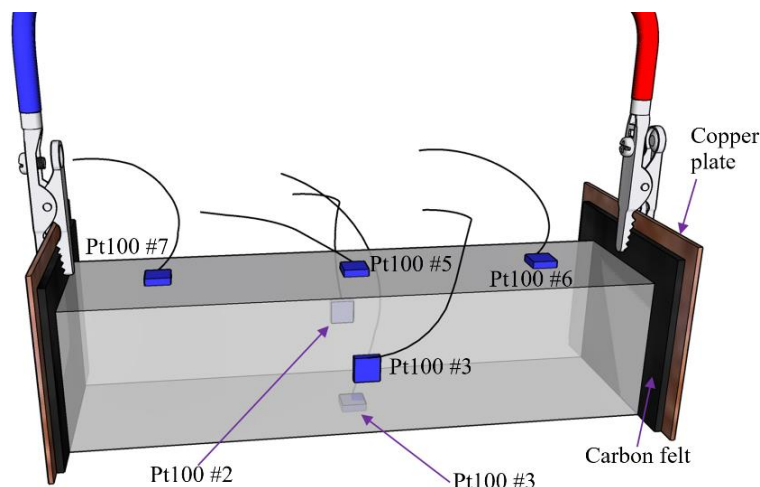


Figure 3. Schematic of a $4 \times 4 \times 16 \text{ cm}^3$ specimen prepared for testing.

Temperature changes on the surface of the samples were continuously recorded using 6 resistance-type Pt-100 temperature detectors connected to a data logger, and two additional Pt-100 sensors were placed to control the ambient temperature. The heating tests were performed by applying different voltages. The higher the applied voltage, the higher the temperature recorded. Different voltages were applied with a direct current (DC) power supply and an alternating current F5V power supply (AC, at 50 Hz). In both cases, the electrical current was measured with Keithley2002 digital multimeters.

3. RESULTS

3.1 Results of strain sensing tests at different temperatures.

The influence of temperature in the range of $0 \text{ }^\circ\text{C}$ to $60 \text{ }^\circ\text{C}$ was studied in isolated tests. Table 1 summarizes the relevant parameters of the tests performed on different days for $0 \text{ }^\circ\text{C}$, $20 \text{ }^\circ\text{C}$, $40 \text{ }^\circ\text{C}$, and $60 \text{ }^\circ\text{C}$. The specimens were naturally returned to room temperature, and the next temperature test was conducted the following day.

Table 1. Effect of temperature on different electromechanical parameters during strain sensing tests: electrical resistivity, elastic modulus, gauge factor, and Pearson's R^2 coefficient of linear regression.

Temperature	Electrical Resistivity (ohm·cm)	Elastic Modulus (GPa)	Gauge Factor (FG)	R^2
$0 \text{ }^\circ\text{C}$	43.70	26.20	14.30	0.968
$20 \text{ }^\circ\text{C}$	43.80	26.00	17.40	0.971
$40 \text{ }^\circ\text{C}$	44.18	23.60	22.30	0.975
$60 \text{ }^\circ\text{C}$	45.70	23.10	58.80	0.888

A slight increase in resistivity with temperature was observed, from 43.7 Ohm·cm at 0 °C to 45.7 Ohm·cm at 60 °C. Similar findings regarding insignificant changes in conductivity between 50 and 115 °C were reported in another study (Demircilioğlu et al., 2019).

The mechanical response was similar in all tests, with elastic moduli between 23 and 26 GPa, excluding any structural damage during loading or heating processes, (del Moral et al, 2021). However, severe changes in the piezoresistive response (see Figure 4) were observed, and the gauge factor (FG) at 60 °C was four times that at 0 °C. A clear increasing trend in FG was noticed upon heating, particularly at the highest temperature level. No specific measures were taken to prevent moisture exchange between the samples and the environment. Figure 4 graphically shows the gauge factors at different tested temperatures.

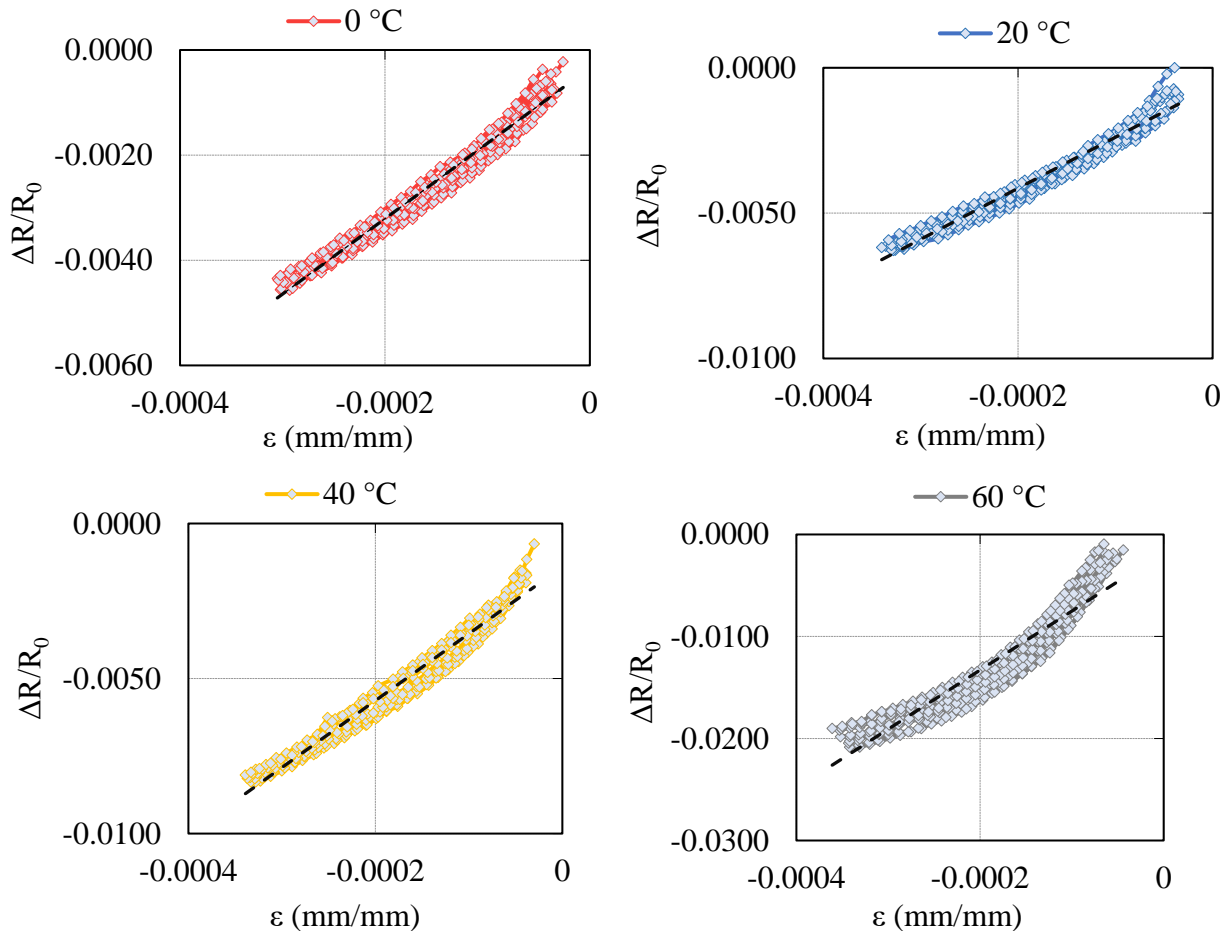


Figure 4. Piezoresistive response of 1% NTC and 5% ABG1010 paste at different temperatures: 0 °C, 20 °C, 40 °C, and 60 °C. Resistance changes against deformation are represented to obtain the gauge factor.

Previous research by Gomis et al. (2015) identified a turning point in these moisture changes at 60 °C. During heating tests, it was observed that water in the pores of cement materials might undergo a state change and begin to evaporate. This alteration of the pore solution could have affected the balance between electrolytic and electronic conduction, enhancing the strain sensing performance in tests after slight drying (Allam et al., 2020; Chung, 2004; Vilaplana et al., 2013).

Moreover, as suggested by Shifeng et al. (2007), temperature can increase the tunnel effect below 100 °C, as electrons convert thermal energy into kinetic energy. Beyond the 100-130 °C limit, higher resistivity values are obtained due to internal pore pressure from increasing water vapor.

In our case, the specimens were heated to a maximum of 60 °C, resulting in surface drying. Consequently, electron mobility increased due to better electronic conduction and the tunnel effect, which may have resulted in enhanced piezoresistive response at these temperatures.

3.2 Results of heating tests.

Figure 5 shows the results obtained for cement paste with 1% CNT and 5% ABG1010 under a 20V AC and DC voltage. The average sample temperatures for both tests in °C and the monitored current (dashed lines) in amperes (A) are presented. In these tests, a temperature increase of +17 °C for both types of current was achieved, which could be sufficient for de-icing systems with ambient temperatures above -15 °C.

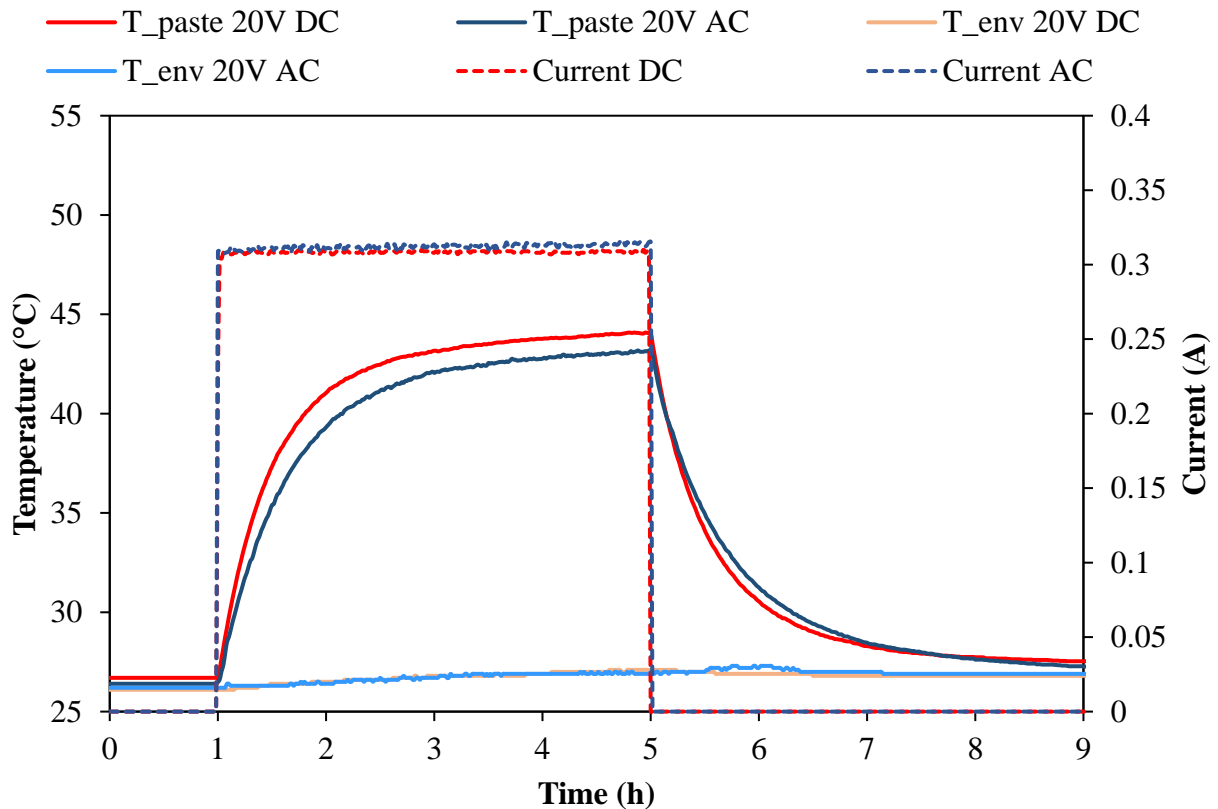


Figure 5. Ambient temperature (T_{env}), specimen's average temperature (T_{paste}), both in °C, and monitored current (dashed lines), in A, versus time (in hours), for heating tests of cement paste in AC and DC with a fixed voltage of 20 V.

Figure 6 shows the temperature of six heating tests with three different samples from different mixtures with the same voltage (40V) in DC and AC. As can be seen, the results are very consistent, confirming reproducibility (same behavior of different samples under the same test).

As can be seen, doubling the applied voltage implies doubling the electric current, which implies a constant resistivity of the compounds in the temperature range shown (Farcas et al., 2021). On the other hand, the maximum temperature reached at 40 V (AC and DC) is approximately 3.3 times higher than the maximum temperature reached at 20 V (AC and DC).

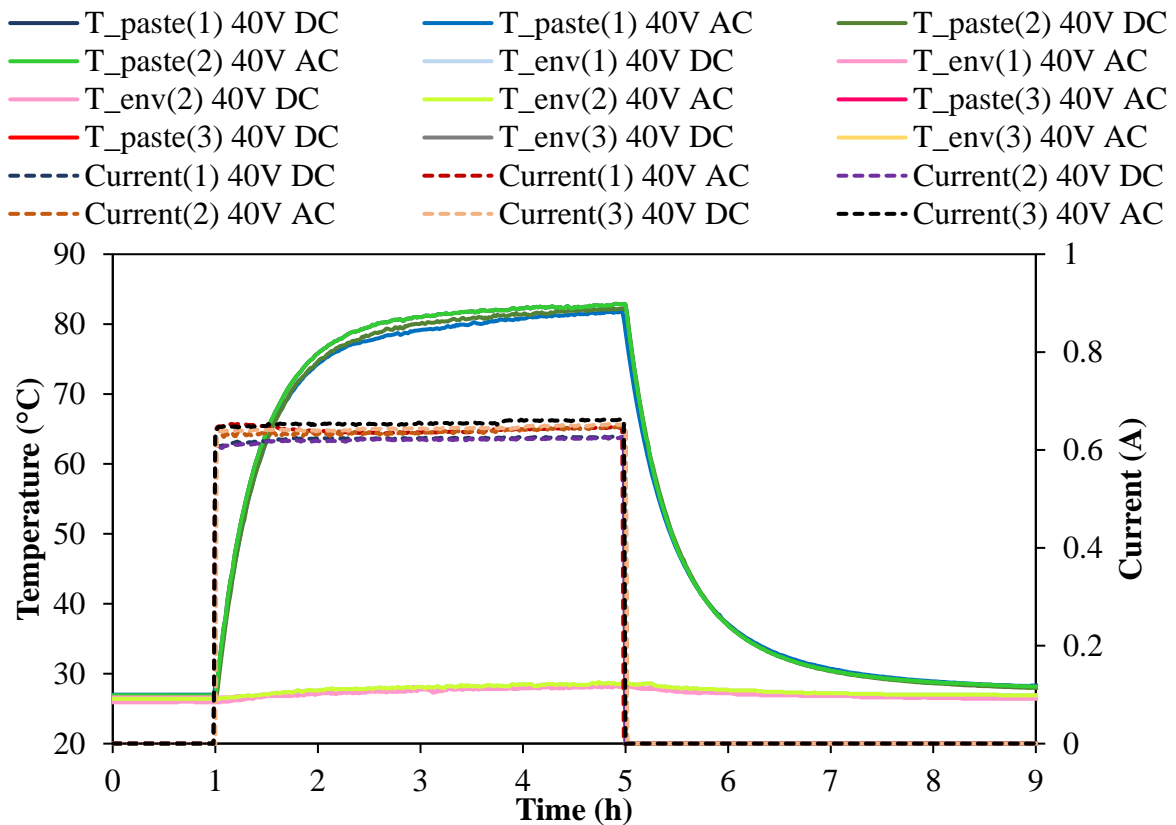


Figure 6 Ambient temperature (T_{env}), specimen’s average temperature (T_{paste}), both in $^{\circ}\text{C}$, and monitored current (dashed lines), in A, versus time (in hours), for heating tests of cement paste in AC and DC with a fixed voltage of 40 V.

Table 2. Summary of electrical characteristics (resistivity, type of current, and applied voltage), temperature variation, and average power.

Resistivity (ohm·cm)	AC/DC	Voltage (V)	Current (A)	ΔT ($^{\circ}\text{C}$)	Average Power (W/m^2)
67	DC	20	0.33	17.10	304
64	AC	20	0.31	17.00	310
64	DC	40	0.64	53.60	1267
67	DC	40	0.62	53.20	1228
67	DC	40	0.62	54.30	1224
66	AC	40	0.63	54.40	1230
64	AC	40	0.64	54.80	1273
63	AC	40	0.65	55.70	1294

Table 2 summarizes the electrical characteristics (resistivity, type of current, and applied fixed voltage), temperature variation, and the energy characteristic, the average power, of the heating tests. In all cases, significant temperature increases can be obtained with relatively small voltage and electric current. Indeed, the type of current applied does not seem to play a significant role in the thermal behavior and energy performance of this material. The resistivity of the samples remains stable under all conditions.

4. CONCLUSIONS

- The feasibility of using cement paste sensors for strain sensing at different temperatures has been successfully demonstrated.
- A slight increase in resistivity with temperature was observed in the strain sensing tests. Furthermore, the increase in temperature (between 0 and 60 °C) led to higher gauge factor (FG) values.
- The feasibility of the heating function in electrically conductive cement pastes with the addition of 1% CNT + 5% ABG1010 has been verified, through the application of both direct current (DC) and alternating current (AC), with negligible differences in the behavior of both currents.
- The results have shown that cement paste samples applied with a 20 V voltage could increase their temperature by +17 °C. Therefore, these compounds would be feasible for de-icing and prevention applications in locations with an ambient temperature of -15 °C.

5. ACKNOWLEDGMENTS

This research was made possible thanks to the funding received from the European funds of the Grant Agreement 760940 MASTRO project.

6. REFERENCES

- Allam, H., Duplan, F., Clerc, J. P., Amziane, S., Burtschell, Y. (2020). *About electrical resistivity variation during drying and improvement of the sensing behavior of carbon fiber-reinforced smart concrete*. In *Construction and Building Materials* (Vol. 264). <https://doi.org/10.1016/j.conbuildmat.2020.120699>
- Baeza, F. J., Galao, O., Zornoza, E., Garcés, P. (2013a). *Effect of aspect ratio on strain sensing capacity of carbon fiber reinforced cement composites*. *Materials and Design*, 51, 1085–1094. <https://doi.org/10.1016/j.matdes.2013.05.010>
- Baeza, F. J., Galao, O., Zornoza, E., Garcés, P. (2013b). *Multifunctional cement composites strain and damage sensors applied on reinforced concrete (RC) structural elements*. *Materials*, 6(3), 841–855. <https://doi.org/10.3390/ma6030841>
- Baeza, F. J., Ivorra, S., Bru, D., Varona, F. B. (2018). *Structural health monitoring systems for smart heritage and infrastructures in Spain*. *Intelligent Systems, Control and Automation: Science and Engineering*, 92, 271–294. https://doi.org/10.1007/978-3-319-68646-2_12
- Banthia, F. A. and N. (n.d.). *Carbon Fiber-Reinforced Cementitious Composites for Tensile Strain Sensing*. *ACI Materials Journal*, 114(1). <https://doi.org/10.14359/51689486>
- Camacho-Ballesta, C., Zornoza, E., Garcés, P. (2016). *Performance of cement-based sensors with CNT for strain sensing*. *Advances in Cement Research*, 28(4), 274–284. <https://doi.org/10.1680/adcr.14.00120>
- Carmona, J., Climent, M.-Á., Antón, C., De Vera, G., Garcés, P. (2015). *Shape Effect of Electrochemical Chloride Extraction in Structural Reinforced Concrete Elements Using a New Cement-Based Anodic System*. In *Materials* (Vol. 8, Issue 6). <https://doi.org/10.3390/ma8062901>
- Chung, D. D. L. (1998). *Self-monitoring structural materials*. 22.
- Chung, D. D. L. (2004). *Self-heating structural materials*. In *Smart Materials and Structures* (Vol. 13, Issue 3, pp. 562–565). <https://doi.org/10.1088/0964-1726/13/3/015>

- del Moral, B., Galao, Ó., Antón, C., Climent, M. A., Garcés, P. (2013). *Viabilidad de utilización de una pasta de cemento con nanofibras de carbono como ánodo en la extracción electroquímica de cloruros en hormigón*. *Materiales de Construcción*, 63(309), 39–48. <https://doi.org/10.3989/mc.2012.03111>.
- del Moral, B., Baeza, F.J., Navarro, R., Galao, O., Zornoza, E., Vera, J., Farcas, C., Garcés, P. *Temperature and humidity influence on the strain sensing performance of hybrid carbon nanotubes and graphite cement composites*. *Construction and Building Materials* 284 (2021) 122786. <https://doi.org/10.1016/j.conbuildmat.2021.122786>.
- Demircilioğlu, E., Teomete, E., Schlangen, E., Baeza, F. J. (2019). *Temperature and moisture effects on electrical resistance and strain sensitivity of smart concrete*. In *Construction and Building Materials* (Vol. 224, pp. 420–427). <https://doi.org/10.1016/j.conbuildmat.2019.07.091>
- Ding, Y., Chen, Z., Han, Z., Zhang, Y., Pacheco-Torgal, F. (2013). *Nano-carbon black and carbon fiber as conductive materials for the diagnosing of the damage of concrete beam*. *Construction and Building Materials*, 43, 233–241. <https://doi.org/10.1016/j.conbuildmat.2013.02.010>
- Farcas, C., Galao, O., Navarro, R., Zornoza, E., Baeza, F. J., Del Moral, B., Pla, R., Garcés, P. (2021). *Heating and de-icing function in conductive concrete and cement paste with the hybrid addition of carbon nanotubes and graphite products*. *Smart Materials and Structures*, 30(4). <https://doi.org/10.1088/1361-665X/abe032>
- Galao, O., Baeza, F. J., Zornoza, E., Garcés, P. (2014). *Strain and damage sensing properties on multifunctional cement composites with CNF admixture*. *Cement and Concrete Composites*, 46, 90–98. <https://doi.org/10.1016/j.cemconcomp.2013.11.009>
- Gomis, J., Galao, O., Gomis, V., Zornoza, E., Garcés, P. (2015). *Self-heating and deicing conductive cement. Experimental study and modeling*. *Construction and Building Materials*, 75, 442–449. <https://doi.org/10.1016/j.conbuildmat.2014.11.042>
- Han, B., Ding, S., Yu, X. (2015). *Intrinsic self-sensing concrete and structures: A review*. *Measurement*, 59, 110–128. <https://doi.org/10.1016/j.measurement.2014.09.048>
- Li, H. N., Li, D. S., Song, G. B. (2004). *Recent applications of fiber optic sensors to health monitoring in civil engineering*. *Engineering Structures*, 26(11), 1647–1657. <https://doi.org/10.1016/j.engstruct.2004.05.018>
- Liu, Q., Schlangen, E., García, Á., van de Ven, M. (2010). *Induction heating of electrically conductive porous asphalt concrete*. *Construction and Building Materials*, 24(7), 1207–1213. <https://doi.org/10.1016/j.conbuildmat.2009.12.019>
- Materials, C., Publishers, K. A. (2001). *Functional properties of cement-matrix*. 6, 1315–1324.
- Shifeng, H., Dongyu, X., Jun, C., Ronghua, X., Lingchao, L., Xin, C. (2007). *Smart properties of carbon fiber reinforced cement-based composites*. *Journal of Composite Materials*, 41(1), 125–131. <https://doi.org/10.1177/0021998306063378>
- Song, G., Mo, Y. L., Otero, K., Gu, H. (2006). *Health monitoring and rehabilitation of a concrete structure using intelligent materials*. *Smart Materials and Structures*, 15(2), 309–314. <https://doi.org/10.1088/0964-1726/15/2/010>
- Ubertini, F., Laflamme, S., Ceylan, H., Luigi Materazzi, A., Cerni, G., Saleem, H., D’Alessandro, A., Corradini, A. (2014). *Novel nanocomposite technologies for dynamic monitoring of structures: a comparison between cement-based embeddable and soft elastomeric surface sensors*. *Smart Materials and Structures*, 23(4), 45023. <https://doi.org/10.1088/0964-1726/23/4/045023>
- Ubertini, F., Laflamme, S., D’Alessandro, A. (2016). *Smart cement paste with carbon nanotubes*. In *Innovative Developments of Advanced Multifunctional Nanocomposites in Civil and Structural Engineering* (pp. 97–120). Elsevier. <https://doi.org/10.1016/B978-1-78242-326-3.00006-3>

- Vilaplana, J. L., Baeza, F. J., Galao, O., Zornoza, E., Garcés, P. (2013). *Self-sensing properties of alkali activated blast furnace slag (BFS) composites reinforced with carbon fibers*. *Materials*, 6(10), 4776–4786. <https://doi.org/10.3390/ma6104776>
- Wang, S., Wen, S., Chung, D. (2004). *Resistance Heating Using Electrically Conductive Cements*. *Advances in Cement Research - ADV CEM RES*, 16, 161–166. <https://doi.org/10.1680/adcr.16.4.161.46662>
- Yehia, S., Tuan, C. Y., Ferdon, D., Chen, B. (2000). *Conductive concrete overlay for bridge deck deicing: Mixture proportioning, optimization, and properties*. *ACI Structural Journal*, 97(2), 172–181. <https://www.scopus.com/inward/record.uri?eid=2-s2.0-0034161181&partnerID=40&md5=2b2d7c46c87b0e36654bccde13f559a3>
- Zhang, K., Han, B., Yu, X. (2011). *Nickel particle based electrical resistance heating cementitious composites*. *Cold Regions Science and Technology*, 69(1), 64–69. <https://doi.org/https://doi.org/10.1016/j.coldregions.2011.07.002>